Conference Paper, Published Version

Fujita, Ichiro; Tsutsumi, Shiho; Ando, Takazumi; Tsubaki, Ryota; Okabe, Takeshi

Flood Surface Flow Measurement by STIV in Adverse Conditions for Imaging

FLOOD SURFACE FLOW MEASUREMENT BY STIV IN ADVERSE CONDITIONS FOR IMAGING

Ichiro Fujita[1], Shiho Tsutsumi[2] , Takazumi Ando[2], Ryota Tsubaki[3] and Takeshi Okabe[4]

[1] Professor, Department of Civil Engineering, Kobe University
Rokkodai-cho, Nada-ku, Kobe, 657-8501, Japan, e-mail: ifujita@kobe-u.ac.jp
[2] Graduate student, Department of Civil Engineering, Kobe University
Rokkodai-cho, Nada-ku, Kobe, 657-8501, Japan, e-mail: ifujita@kobe-u.ac.jp
[3] Researcher, Department of Civil Engineering, Nagoya University
Furo-cho, Chikusa-ku, Nagoya, 464-8603, Japan, e-mail: r.tsubaki@civil.nagoya-u.ac.jp
[4] Professor, Department of Civil Engineering, The University of Tokushima
Shinkura-cho, Tokushima, Kobe, 770-8501, Japan, e-mail: okabetak@ce.tokushima-u.ac.jp

ABSTRACT

The non-contact flood flow measurement techniques using video images have become available in the last decade, one of which is the large-scale particle image velocimetry (LSPIV, Fujita, et al. 1998). LSPIV yields successful results for various flood flow measurements such as the Yodo River, the Uono River and rivers in the other countries. However, since the method is based on the imaging techniques, the measurement becomes relatively difficult in adverse imaging conditions such as low light or bad weather conditions. The space-time image velocimetry (STIV, Fujita et al. 2007) is another candidate for surface flow measurements which can yield streamwise velocity distributions more efficiently than LSPIV even in deteriorated image conditions. In this research, the performance of STIV is compared with LSPIV by applying them to the flood flow measurements in two rivers in Japan, the Chigusa River and the Yoshino River, both recorded during the night. It was confirmed that STIV yields reasonable results even in adverse conditions for imaging in which LSPIV is inapplicable due to the condition's severity.

Keywords: surface flow measurement, STIV, LSPIV, image analysis, flood flow

1. INTRODUCTION

River discharge is one of the most important hydrological variables in planning rivers. However, accurate discharge measurement is always a problem when it comes to the measurement during large floods. Conventionally a float method has been used in Japan and Korea in the past several decades, but this method cannot always yield a reasonable result because of the poor tracerbility of floats in vortical flow field or danger during measurements, and so forth. The other problem is that discharge measurement itself has not been performed regularly in relatively small scale rivers, especially the class B Rivers in Japan, in which case the water level rises quickly sometimes more than one meter in half an hour from shallow water depth. Therefore, alternative measurement methods have been developed so far such as Acoustic Doppler current profiler (ADCP), UHF radar (Teague, et al. 2007; Cheng, et al. 2007) ultrasonic wave velocity meter or imaging techniques that uses the idea of particle image velocimetry (PIV, Fujita and Komura, 1994, Aya and Fujita, 2000). The latter three techniques assume that water surface ripples, waviness or image pattern appeared during floods are convected with the local surface velocity or at least with a speed having a close correlation with the surface velocity. Among the above methods, imaging technique is a good candidate for measuring flood velocity or discharge under various conditions rather economically because even a personal camcorder can be used for measurements. The disadvantage of the method is its inability to measure during the night since it uses the visible light reflection from the water surface. The other problem is the effect of weather conditions, in which case the images are sometimes blurred by rain drops and in the worse case the surface pattern itself is destroyed due to strong wind. In this research, in order to overcome the problem associated with night measurements, several measurements were conducted under which deteriorated images might be obtained and the performance of the two imaging methods, LSPIV and STIV are examined in detail.

2. FLOOD MEASUREMENT OF THE CHIGUSA RIVER

Image recording system for CCTV

The Chigusa River is one of the class B Rivers in Hyogo Prefecture in Japan. At the location about 14km from the river mouth, a CCTV system is installed on the right bank as shown in Figure 1. The lower channel width is about 65m and the width of the flood plain is about 40m at the site. Since this system has been used only for the visual inspection of flow about bridge piers or water level, we installed an image storing system for recording water surface images as a sequence of MPG movie files. This system is composed of a one terra-byte hard disk and a hardware controlling the schedule of image recording. In the present case, we setup the system so that one minute of surface image is recorded on the hard disk as a movie file at an interval of ten minutes. With this system, about two-months of consecutive image recording has become possible.

2007 Chigusa River Flood

While recording in July 2007, we succeeded in capturing a sequence of flood event with peak water level occurred during the night. The hydrograph at the site is presented in Figure 2 together with representative surface images at several time zones. In this flood the peak water level is about 3.71m which occurred around 7:30pm on July 14. At this stage, the water level exceeds the flood plain level a small amount. Hence, the width of water surface exceeds the lower channel width at the peak discharge period of the flood and becomes the maximum of 81 m in the present flood.

The problem with the recorded image data is that since the weather is still in heavy rain in the early part of the hydrograph, the image quality is significantly deteriorated to use in the normal image analysis of LSPIV. Figure 2 also indicates that the image quality becomes quite different depending on the time zone. Typical examples of low-quality image are presented in Figure 3. Figure 3(a) indicates the adherence of raindrops on the glass window at the front of camera cover. As these raindrops keep sticking to the filter, the representative image analysis method LSPIV is difficult to apply because LSPIV is

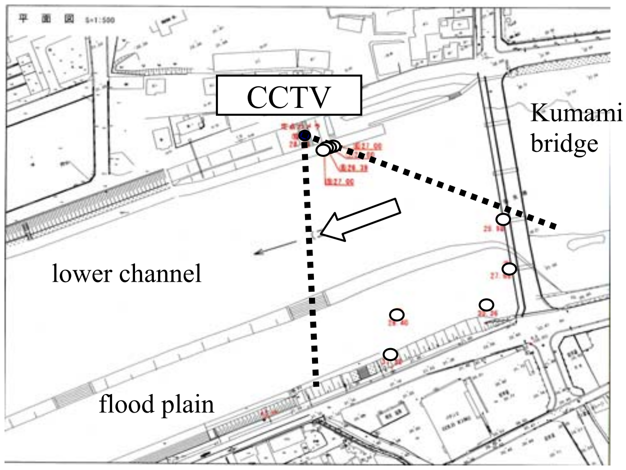

Figure 1 CCTV location at the Chigusa River; filled black circle: CCTV location, white circles: mark points for mapping CRT and physical coordinates

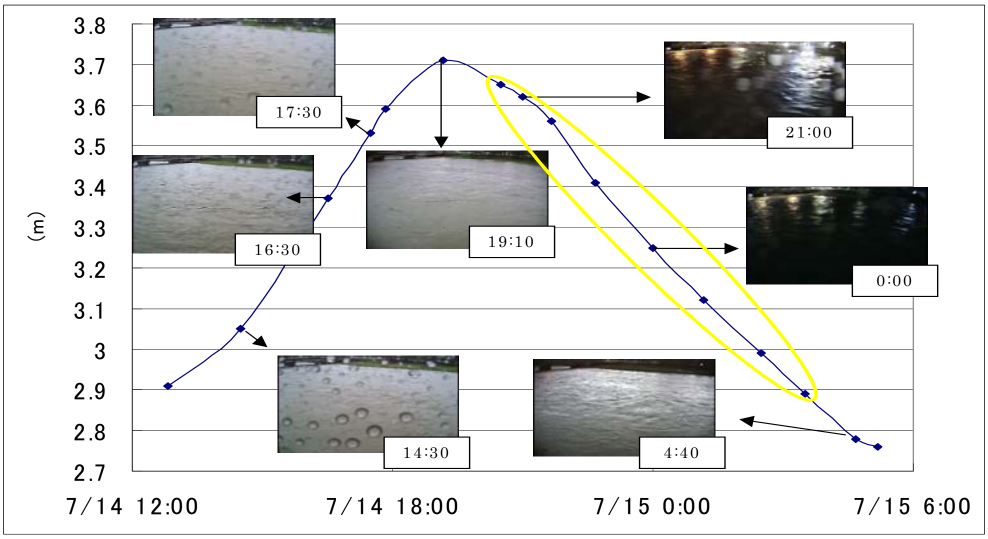

Figure 2 Water level hydrograph and surface images in 2007 Flood

(a) raindrop effect (b) low-light effect with raindrop

Figure 3 Low quality surface images of the Chigusa River flood

based on the pattern matching algorithm. Figure 3(b) is the extreme case in which the water surface area is only partially visible by several lights behind the river with raindrops on the glass cover window. Additionally, frame dropping appears in the movie due to the lack of light intensity coming to the CCTV, because CCTV cameras usually reduce frame rate automatically when the environment light intensity becomes less than a threshold level. In order to extract velocity information as much as possible from such a low-quality movie, we applied STIV to such images and compared them with the LSPIV results.

Application of STIV

In the application of the STIV to the river flow measurement, a line segment such as indicated in Figure 3 is set parallel to the main flow direction and the evolution of the image intensity in the line segment is represented as a space-time image (STI) as shown in Figure 4. In this example the physical length of the line segment is 9.8m while the vertical length corresponds to the ten seconds of image, 300 pixels in STI. The physical length scale at the water surface can be calculated once the mapping relation between the physical and the CRT coordinates are established together with the water level information. Incidentally, the white circles indicated in Figure 1 are the mark points used for establishing the relation. It is evident from Figure 4 that a striped pattern, with its angle indicating the mean velocity passing through the line segment, appears in the space-time image. In Figure 4(a) the dark vertical thick line corresponds to the raindrops adhered to the filter during the measurement. However, the general inclined pattern is clearly observable. On the other hand, in Figure 4(b), the image is extremely deteriorated due to the scarcity of enough light as mentioned previously. Usually, the conventional CCTV camera changes its recording mode from the normal one to a frame accumulating mode in order to make the image visible even in the dark condition, which results in the frame dropping. The problem with this mode is that the generated STI includes stair-like patterns as a result of the frame dropping. However, at least it is possible to recognise the gradient of the inclined pattern by visual inspection as plotted in Figure 4(b). Therefore, by applying the same procedure for line segments covering whole width of the river, the surface velocity distribution can be calculated, from which river discharge can be estimated with the information of bathymetry at the section.

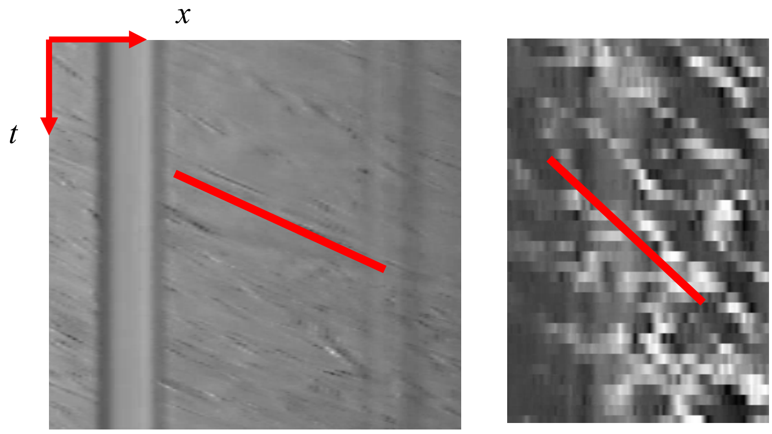

(a) (b)

Figure 4 Space-time images for search line in Fig.1: horizontal =9.6m(left),9.8m(right), vertical = 10.0s

Outline of STIV

The STIV (Fujita et al. 2007b) is the algorithm to calculate automatically the mean gradient or image orientation appeared in the space-time image by image analysis. Therefore if it becomes possible to extract image gradients under various imaging conditions including the worst condition as mentioned previously, a robust measurement system could be established. According to the STIV algorithm, the orientation angle ϕ can be calculated by the relation,

$$\tan 2\phi = \frac{2J_{xt}}{J_{tt} - J_{xx}}, \tag{1}$$

where

$$J_{xx} = \int_A \frac{\partial g}{\partial x}\frac{\partial g}{\partial x}dxdx, \quad J_{xt} = \int_A \frac{\partial g}{\partial x}\frac{\partial g}{\partial t}dxdt, \text{ and } J_{tt} = \int_A \frac{\partial g}{\partial t}\frac{\partial g}{\partial t}dtdt, \tag{2,3,4}$$

g is the distribution of image intensity in STI and A is the local window area in STI. Another important parameter is termed coherency C, which is a measure of coherence of image pattern and defined by

$$C = \frac{\sqrt{(J_{tt} - J_{xx})^2 + 4J^2{}_{xt}}}{J_{xx} + J_{tt}}. \tag{5}$$

The value of coherency changes from 0 to 1. For ideal local orientation the value becomes one and for an isotropic gray image it becomes zero. Therefore it is possible to pickup only the clear orientation information by using the coherence value as a weighting function:

$$\bar{\phi} = \int \phi C(\phi)d\phi./\int C(\phi)d\phi. \tag{6}$$

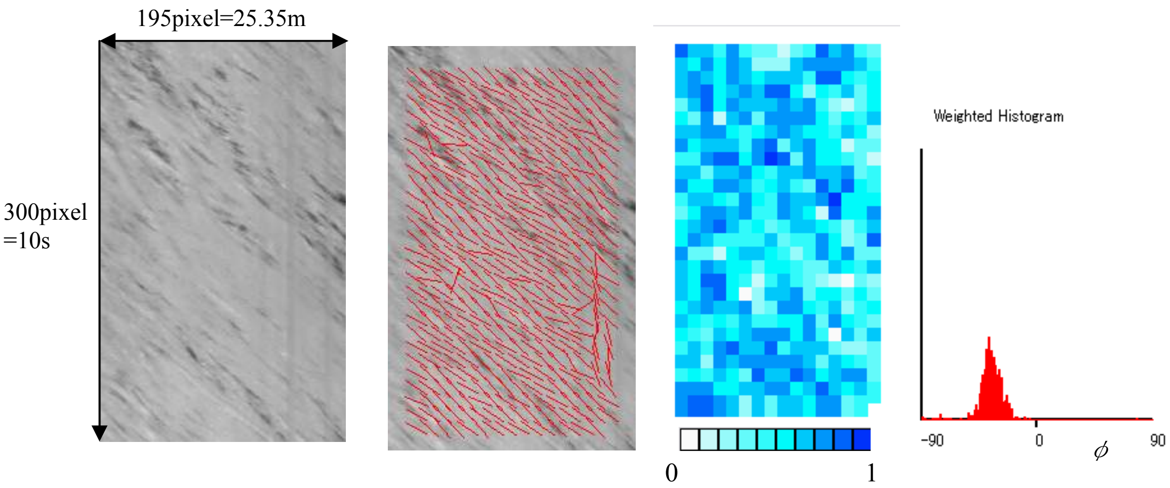

(a) STI (b) STI with orientation vectors (c) coherency (d) histogram

Figure 5 STIV procedure

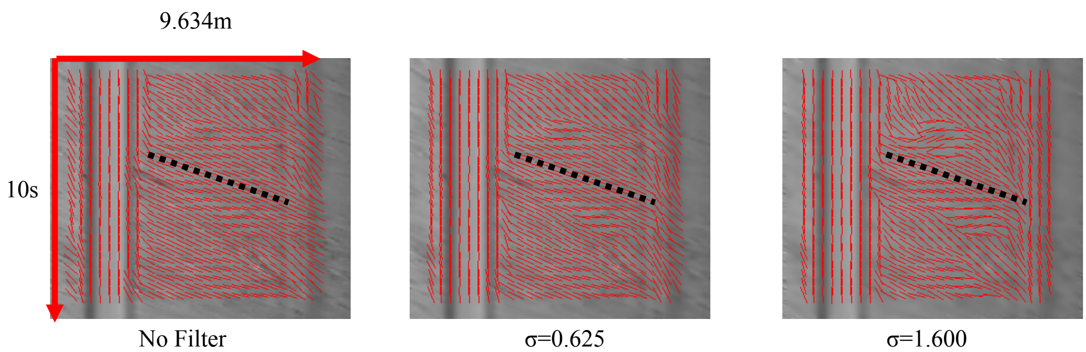

(a) orientation vectors

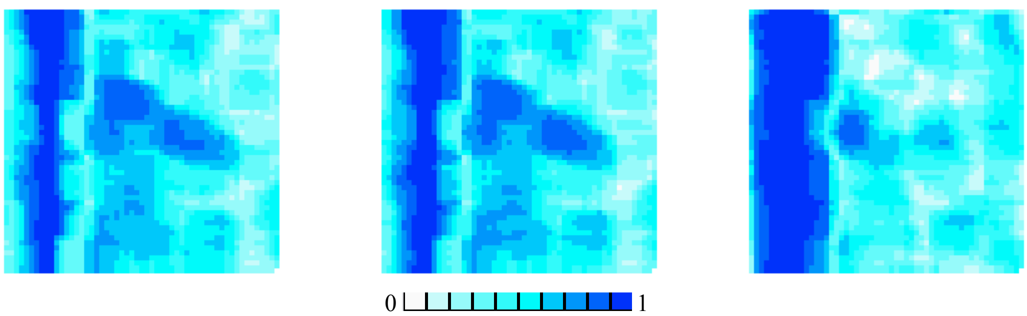

(b) coherency

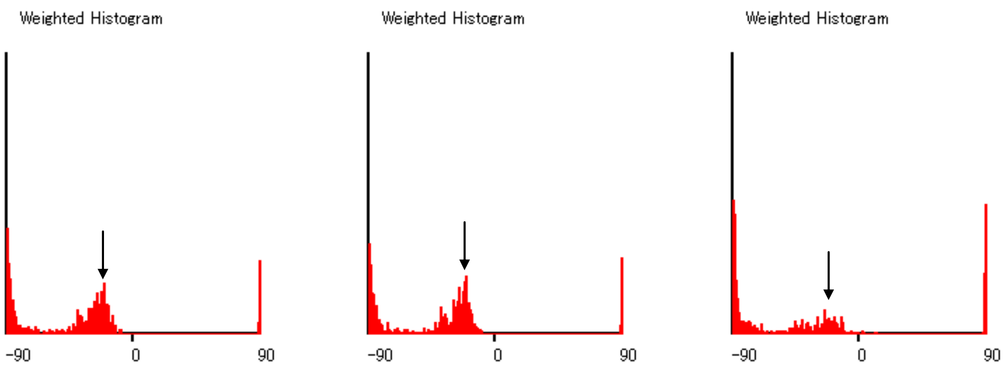

(c) histogram

Figure 6 Effects of smoothing filter

An example of STIV procedure is presented in Figure 5. The STI is divided into sub-windows and for each window an orientation vector is calculated from eq.(1), with a result presented in Figure 5(b). Subsequently by using the corresponding coherency distribution shown in Figure 5(c) as a weighting function, a histogram for the orientation angles is obtained, from which the mean orientation angle is calculated by eq.(6). In the application of STIV to the actual space-time image, it is appropriate to apply a smoothing filter to STI before calculating orientation vector to improve the accuracy, because application of Gaussian filter of proper size would improve the coherency values as shown in Figure 6. In this case, the proper size is the one with a standard deviation σ of 0.625 pixels. Figure 6 also suggests over smoothing would decrease the level of coherency distribution. From the histogram of Figure 6(c), it is easy to separate the effect of raindrop because the histogram provides two peaks, only one of which corresponds to the surface flow. In addition, the arrow shown in Figure 6(c) indicates the orientation angle by visual inspection presented as dotted line in Figure 6(a). This angle corresponds well with the peak angle in the histogram.

Application to deteriorated images

Application of STIV algorithm to deteriorated STI previously presented in Figure 4(b) is shown in Figure 7. Apparently, no filtering results in the generation of horizontal orientation vector due to the frame dropping. With increasing the size of the Gaussian filter

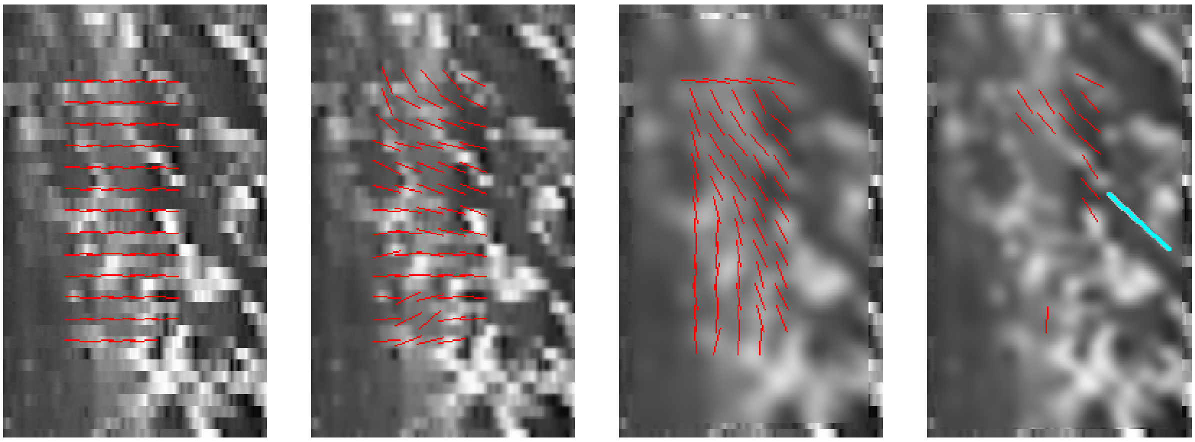

No filter σ=0.625 σ=2.56 σ=2.56, c>0.3

Figure 7 STIV application to deteriorated STI

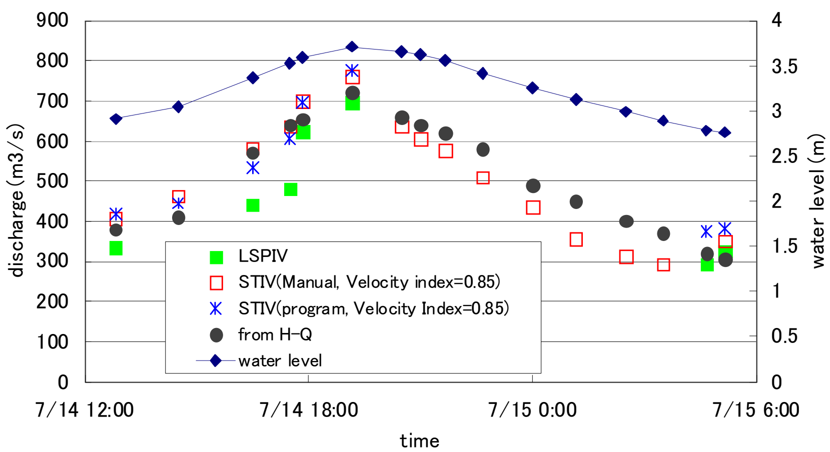

Figure 8 Comparison of discharge hydrographs

reasonable orientation vectors begin to appear. In the present case, σ=2.56 yielded appropriate orientation angles. Further, by using the coherency as a threshold level, it becomes possible to pickup vectors almost parallel to the one by visual inspection as indicated in Figure 7.

Finally, the discharge hydrographs obtained by various methods are compared in Figure 8. In the analysis, about one minute of image data are used to obtain the mean velocity data. It is apparent that LSPIV yields underestimated data for the case of raindrop adherence in the rising stage. On the other hand, STIV yields reasonable data comparable to that estimated from the stage discharge relationship. However, since STIs during the night include various noises difficult to filter out only by using the coherency-weighted histogram. Hence, the orientation angles had to be measured with visual inspection in the present research. In the visual inspection, a line segment considered parallel to the average orientation of the pattern is drawn manually on the STI by a mouse operation and the orientation angle is calculated from the gradient of the line segment. The discharge hydrographs thus obtained also generated reasonable time variation as shown in Figure 8.

3. FLOOD MEASUREMENT OF THE YOSHINO RIVER

Outline of flood measurement

In the case of the Yoshino River flood, on the other hand, no CCTV station is available at the measuring section located about 64km from the river mouth (Fujita et al. 2007a); therefore we went to the measurement site and videotaped the flood image by a personal camcorder under the infra-red mode while scanning the river surface with a strong portable search light waving back and forth. Since this site is located in the mountainous area, no light source is available other than the halogen light source we brought. However, with the above combination of light source and recording mode, surface flow was made visible as shown in Figure 8. The target flood occurred July 14, 2007 and we started the measurement from 22:30, 23:08, and 0:12, 0:54 the next day. Each measurement continued for several minutes. The small flags shown in Figure 9 are the mark points for establishing image mapping between CRT and physical coordinates.

Figure 9 Infra-red image made visible with halogen search light

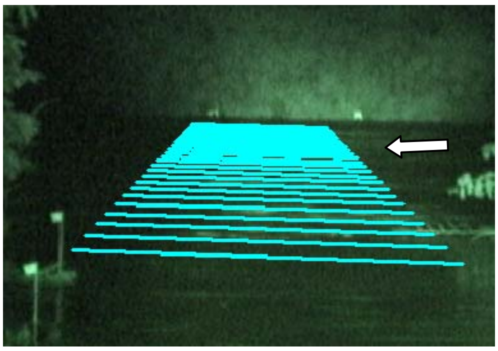

(a) CRT coordinates

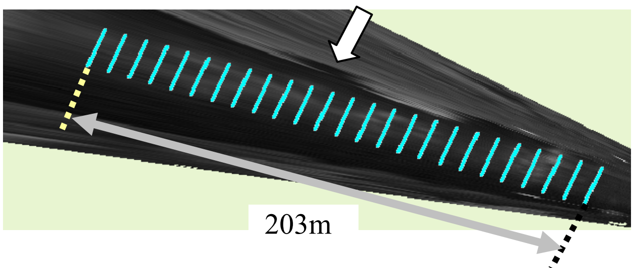

(b) Physical coordinates

Figure 10 Arrangement of line segments

Application of STIV

In the application of the STIV to the surface image, we changed the length of the line segments in CRT coordinates so that their physical lengths become the same in the transformed image as shown in Figure 10. The physical length of the line segment here is set at 15.38m and the farthest and nearest line segments are 278.3m and 74.5m from the camera location, respectively. The angle of repose is 6.78degrees in the nearest location and 1.82degrees in the farthest location. The problem with the image recording is that even though the image was made visible there occurred frame dropping in STI as indicated in Figure 11(a); therefore we applied a relatively large sized Gaussian filter, σ=2.5 pixels for example, to the STI as presented in Figure 11(b). With this filtering, more reliable orientation vectors were obtained.

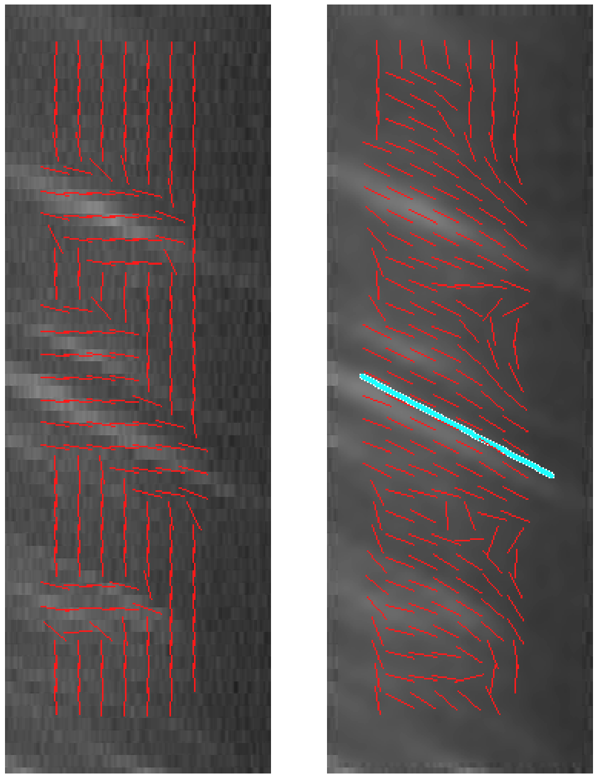

(a) original (b) filtered

Figure 11 Application of Gaussian filter; σ= 2.5 pixel

Figure 12 compares the surface velocity distributions obtained by visual inspection and STIV algorithm. In the present STIV, orientation angles with coherency values more than 0.2 are picked up for weighting. Although there still remains some scatter, transverse velocity distributions with the maximum surface velocity of about 5m/s are calculated fairly well. As a comparison, LSPIV is applied to the transformed images as shown in Figure 13. It is clearly seen that LSPIV yields erroneous values in most of the locations. This result can be easily predicted since, due to the frame dropping, the time interval between the images used in LSPIV does not always gives a proper

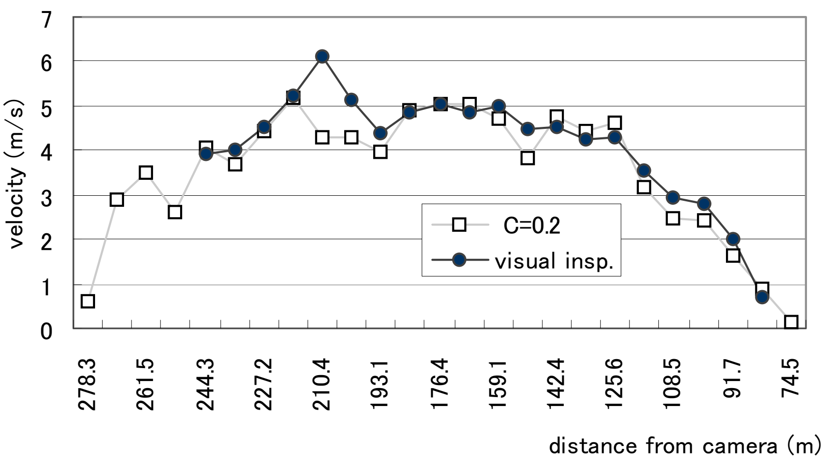

Figure 12 Surface velocity distributions at 23:12 July 14, 2007

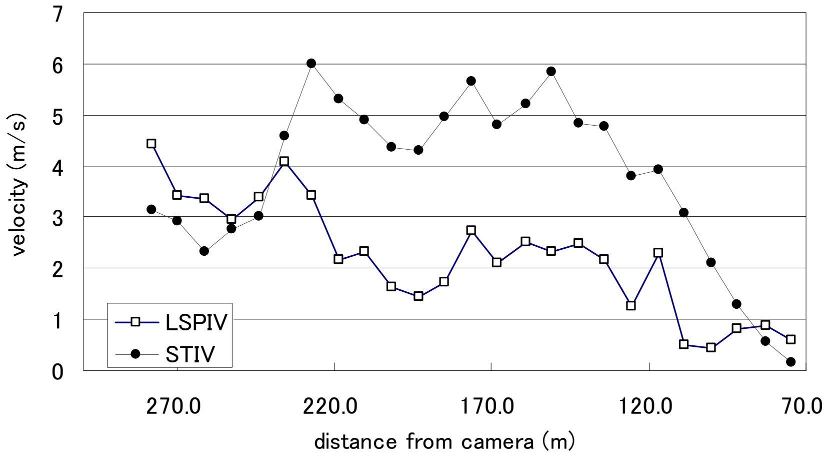

Figure 13 Comparison of STIV and LSPIV at 0:12 July 15, 2007

value. Therefore, in order to apply LSPIV to such site as the present case, a high-sensitivity video camera would be required to acquire a reasonable result.

4. CONCLUSIONS

One of the non-intrusive measurement techniques, the space-time image velocimetry (STIV) developed by the authors, is applied to the flood flows occurred in the Chigusa River and the Yoshino River. The conditions for measurement were not appropriate for imaging techniques, with raindrop adherence to the lens filter or low light conditions entailing the frame dropping which yield fatal errors in LSPIV. In the present research, it was made clear that most of those problems can be overcome by applying STIV algorithm to the space-time image (STI) and the results confirmed the versatility of the STIV in adverse conditions for imaging. However, in some cases with worst imaging conditions, visual inspection of orientation angles of STI had to be conducted since the STIV algorithm yielded erroneous results accompanying flat histogram pattern with no predominant value. Further research is required to extract more reliable orientation angles even when there appears a subtle evidence showing the convection of surface flow.

ACKNOWLEGEMENTS

We are grateful for the support by the NTT Infranet coorpration in acquiring the surface images of the Chigusa River.

REFERENCES

Aya, S. and Fujita, I.(2000), Refinement of LSPIV technique for monitoring river surface flow,ASCE 2000 *Joint Conference on Water Resources Engineering and Water Resources Planning & Management,*on CDROM.

Cheng, R. T., Burau, J. R., DeRose, J., Barrick, D. E., Teague, C. C. and Lilleboe, P. M. (2007), Measuring Two-dimensional surface velocity distribution using two RiverSondes, *Book of Extended Abstracts, Hydraulic Measurements & Experimental Methods,* pp.184-189.

Fujita, I., and Komura, S. (1994), Application of video image analysis for measurements of river-surface flows, *Annual Journal of Hydraulic Engineering*, Japan Society of Civil Engineers, 38, pp.733-738 (in Japanese).

Fujita, I., Muste, M. and Kruger, A. (1998), Large-scale particle image velocimetry for flow analysis in hydraulic engineering applications, *Journal of Hydraulic Research*, Vol.36, No.3, pp.397-414.

Fujita, I., Tsubaki, R. and Okabe, T. (2007a), Measurements of flood discharge by using space time image velocimetry with a high resolution video camera, *Proceedings of 32nd IAHR Congress*, on CDROM.

Fujita, I., Watanabe, H. and Tsubaki, R. (2007b), Development of a non-intrusive and efficient flow monitoring technique: The space time image velocimetry (STIV), *International Journal of River Basin Management,* 5(2), pp.105-114.

Teague, C. C., Barrick, D. E., Lilleboe, P. M., and Cheng, R.T. (2007), RiverSonde: measuring river surface velocity with UHF Radar, *Book of Extended Abstracts, Hydraulic Measurements & Experimental Methods,* pp.178-183.